

# Whom We Trust, What We Fear: COVID-19 Fear and the Politics of Information

Daniele Baccega<sup>1</sup>, Paolo Castagno<sup>1</sup>, Antonio Fernández Anta<sup>2,3</sup>, Juan Marcos Ramirez<sup>2</sup>, Matteo Sereno<sup>1</sup>

<sup>1</sup> Department of Computer Science, University of Turin, Turin, Italy

<sup>2</sup> IMDEA Networks Institute, Madrid, Spain

<sup>3</sup> IMDEA Software Institute, Madrid, Spain

daniele.baccega@unito.it, paolo.castagno@unito.it, antonio.fernandez@imdea.org, juan.ramirez@imdea.org, matteo.sereno@unito.it

## Abstract

The COVID-19 pandemic triggered not only a global health crisis but also an *infodemic*, an overload of information from diverse sources influencing public perception and emotional responses. In this context, fear emerged as a central emotional reaction, shaped by both media exposure and demographic factors. In this study, we analyzed the relationship between individuals' self-reported levels of fear about COVID-19 and the information sources they rely on, across nine source categories, including medical experts, government institutions, media, and personal networks. In particular, we defined a score that ranks fear levels based on self-reported concerns about the pandemic, collected through the Delphi CTIS survey in the United States between May 2021 and June 2022. We found that both fear levels and information source usage closely follow COVID-19 infection trends, exhibit strong correlations within each group (fear levels across sources are strongly correlated, as are patterns of source usage), and vary significantly across demographic groups, particularly by age and education. Applying causal inference methods, we found that among age, education, and information source, the latter is the most influential factor affecting individuals' fear levels. We further quantified the impact of different information sources on fear by estimating the average treatment effect, indicating how each source alters fear relative to a control. Furthermore, we demonstrated that information source preferences can reliably match the political orientation of U.S. states. These findings highlight the importance of information ecosystem dynamics in shaping emotional and behavioral responses during large-scale crises.

## Introduction

The COVID-19 pandemic represented a global health crisis of unprecedented scale and complexity. At the same time, it generated an *infodemic*—a rapid and overwhelming surge of information from a wide range of sources (Cinelli et al. 2020). As individuals sought clarity and guidance, they turned to news media, social platforms, government announcements, and public health organizations. The credibility, consistency, and framing of these sources played a critical role in shaping public understanding of the threat. Additionally, they influenced emotional responses across populations (Jones, Mougouei, and Evans 2021; Lu et al. 2021).

Copyright © 2026, Association for the Advancement of Artificial Intelligence (www.aaai.org). All rights reserved.

In this context, fear emerged as one of the most prominent psychological responses to the pandemic (Coelho et al. 2020). This emotion was not driven solely by the objective health threat, but also by the volume, tone, and perceived trustworthiness of the information consumed. The impact of these information sources on fear varied across different demographics. Differences in age, education, gender, and socioeconomic status significantly shaped how individuals selected, interpreted, and trusted various sources (Nino et al. 2021). These disparities highlight the necessity of accounting for both the nature of the information disseminated and the characteristics of the recipients when evaluating the psychological impact of information exposure.

Furthermore, information played a dual role during the crisis: it served both as a practical resource for guiding health-related decisions and as a symbolic indicator of political identity and civic orientation. The choice to trust or dismiss specific sources frequently mirrored broader ideological affiliations, shaping not only individual behaviors but also the level of collective trust in public institutions. Against this backdrop, the risks posed by misinformation—particularly when it stemmed from institutional or otherwise authoritative sources—became especially salient. Perceptions of inconsistency, politicization, or unreliability in official communications had the potential to undermine not only adherence to public health guidance but also confidence in democratic institutions. Understanding how various demographic groups navigated this complex informational environment is, therefore, critical for designing communication strategies that bolster both public health outcomes and civic trust in future crises.

## Contributions

Our main contributions are as follows—summarized in Figure 1. First, using statistical tests and correlation analyses on U.S. data, we quantify the influence of different information sources on individuals' COVID-19-related fear levels, and similarly assess differences in information source usage across the population. Second, we investigate how demographic factors—specifically age and education—not only affect emotional responses but also significantly shape information-seeking behavior and trust, revealing notable patterns across population groups. Third, through a causal inference model, we compare the relative impact of age,

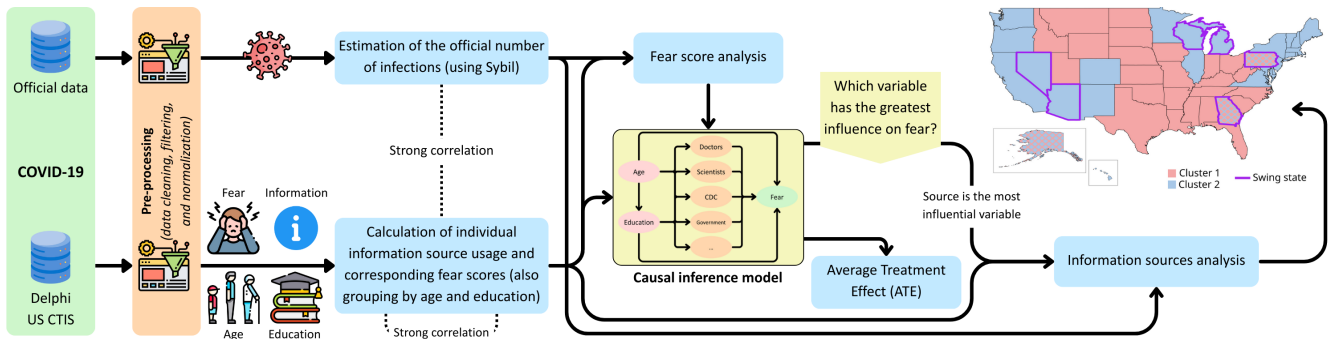


Figure 1: Schematic representation of our study.

education, and information source on fear, finding that information source is the most influential driver. We then estimate the average treatment effect (ATE) to quantify how each source alters fear compared with a control source. Finally, building on this, we apply K-means, spectral, and hierarchical clustering to group U.S. states based on their residents’ reliance on different types of information. Remarkably, the resulting clusters exhibit a strong alignment with state-level political orientation—specifically, whether a state tends to lean Democratic or Republican. Collectively, our findings underscore the critical role of information sources in shaping population emotional responses to large-scale crises. They also highlight the dangers of misinformation—particularly when disseminated by institutional or authoritative entities—which can distort public perception, exacerbate fear, and undermine trust in democratic institutions.

This article is organized as follows. The *Related work* section reviews prior research on *fake news*, misinformation, and COVID-19–related fear, highlighting key findings and existing gaps. The *Data* section describes our data sources and the construction of the indices used in the analysis. The *Methods* section presents the methodology, including correlation analysis, causal inference, and clustering. The *Results* section examines variation in fear levels across information sources and demographic groups, as well as variation in information source usage across demographics, and identifies patterns of information reliance across the U.S. Finally, the *Conclusion* section summarizes the main findings and discusses their broader implications.

## Related work

A growing body of research has examined the spread of *fake news* and misinformation during the COVID-19 pandemic and their psychological consequences—particularly the prevalence and dynamics of fear. This fear has been fueled by false or low-credibility information presented as legitimate news which has also undermined trust in vaccines and preventive measures and contributed to a global *infodemic* (Caceres et al. 2022).

Evidence shows that information sources strongly shape risk perceptions and emotional responses. In Portugal, scientific sources had greater effects on perceived personal and societal risk than general media, and trust in science height-

ened perceived vulnerability, while trust in social media reduced it (Entradas 2022). In the U.S., socioeconomic and political divisions shaped information-seeking behaviors: individuals with higher education and digital skills accessed a more diverse range of sources, whereas reliance on conservative media was associated with lower levels of factual knowledge (Reisdorf et al. 2021). Additional analyses of social media behavior show that online discourse around COVID-19 was heavily politicized: an investigation of Facebook posts from users who engaged with anti-government and COVID-denialist narratives before later dying from the virus found that harmful themes were largely propagated within a right-wing political and media ecosystem, with platforms applying only soft moderation measures (Habib and Nithyanand 2023). This underscores both the politicization of COVID-19 information and the role of platform governance in shaping exposure to dangerous narratives.

False information spreads far more rapidly than accurate content on social platforms, largely propagated by superspreaders in ideologically aligned networks. While fact-checking demonstrates limited durability, psychological inoculation strategies employing gamified prebunking show enhanced efficacy in building cognitive resistance (Van Der Linden 2022). These dynamics amplify infectious disease transmission through behavioral mechanisms by promoting harmful practices and undermining prevention. Misinformation persists longer and spreads more readily than factual information, substantially increasing infection rates (Bernardin and Perez-Acle 2025). Additionally, the impact on vaccination intentions is especially pronounced; randomized controlled trials demonstrate that exposure to vaccine misinformation reduces the intent to vaccinate by approximately 6 percentage points relative to factual information, with greater effects for scientifically sounding misinformation and differential impacts across sociodemographic groups (Loomba et al. 2021). Research also shows that misinformation about COVID-19 vaccines is driven by coordinated conspiracy-oriented communities that amplify anti-vaccine narratives and distort scientific evidence, contributing to polarized uptake patterns (Sharma, Zhang, and Liu 2022). Automated approaches to misinformation monitoring also support these findings: neural stance-classification models using graph attention networks can reliably iden-

tify whether social media posts adopt or reject COVID-19 misinformation, revealing consistent patterns in the emotional, lexical, and thematic structure of misinformation uptake (Weinzierl, Hopfer, and Harabagiu 2021). Meanwhile, even a single trusted correction can reduce belief in misinformation (Seo et al. 2022; Miyazaki et al. 2023), emphasizing the importance of timely and credible debunking.

Social media commentary on COVID-19 was largely negative, with anger dominating globally and fear peaking early in the pandemic, later rising only during variant or mortality news. Emotional expression varied by region, with the U.S. showing more anger, African outlets more sadness, and Indian sources more fear. In particular, fear emerges as a central psychological response shaped more by subjective perceptions and social transmission than by epidemiological indicators. Social media analyses reveal that fear expression peaks during early outbreak phases and shows substantial gender differences, with women expressing fear more frequently than men in response to disease-related topics. The temporal dynamics of fear demonstrate marked fluctuations independent of actual disease severity, with daily shares of fear posts significantly elevated during peak COVID-19 periods compared to baseline 2019 levels (Chai et al. 2022). Cross-national longitudinal research finds that roughly 23% of fear variance is explained by micro-level psychological factors—worries about resource shortages, perceived disease vulnerability, germ aversion, and infections in close social circles—while macro-level indicators like case counts, mortality, and restrictions contribute minimally. Individual traits such as age, attachment anxiety, and prior health concerns further shape fear responses, revealing heterogeneous susceptibility and a disconnection between subjective threat perception and objective epidemiological data (Eder et al. 2021). Agent-based models with associative learning reveal that falling fear can trigger new disease waves by reducing protective behavior, which strongly shapes epidemic trajectories. Media campaigns promoting protective actions have minimal impact, suggesting interventions must target the psychological drivers of fear and compliance, not just factual disease information (Retzlaff et al. 2022).

Moreover, early population-level fear modestly predicted later vaccination willingness but was insufficient alone to explain vaccine hesitancy, which involves multiple psychological and risk-perception factors. Demographically, females, healthcare workers, lower-educated, and married individuals showed higher fear, highlighting vulnerable groups needing targeted interventions that address fear alongside vaccine-related beliefs (Oliveira et al. 2023; Mertens et al. 2022; Doshi et al. 2021). Finally, causal inference reveals bidirectional relationships between media exposure, interpersonal communication, and fear of COVID-19. Both media frequency and perceived danger in conversations predict fear, while elevated fear motivates increased media and communication seeking. Counterarguing proves most effective at reducing fear and encourages sustained use, with individuals cycling from avoidance to counterarguing to reappraisal as the pandemic progresses. These adaptive emotion-regulation patterns suggest that targeted interventions addressing maladaptive regulatory pathways prove more effective than uni-

form communication approaches (Li 2022).

Overall, misinformation and fear jointly influence pandemic behavior through interconnected mechanisms. Misinformation spreads rapidly, reduces vaccination intentions, and undermines protective behaviors, while fear—driven largely by subjective perceptions, information exposure, and social context—varies across demographic groups and feeds back into information-seeking patterns. Declining fear can weaken compliance and contribute to renewed outbreaks.

Despite extensive research on misinformation and fear during the COVID-19 pandemic, key gaps remain. The influence of different information sources on fear across demographic groups remains poorly characterized. Additionally, geographic and political influences remain underexplored. Addressing these gaps is critical for designing interventions that effectively mitigate misinformation, target heterogeneous fear responses, and support vulnerable populations. Our study addresses these gaps by employing advanced statistical and causal inference methods to evaluate how demographics and sources of information jointly shape fear responses. Moreover, by clustering U.S. states according to patterns of information source usage and linking these clusters to political orientation, we offer a comprehensive, integrated perspective on the social and contextual determinants of COVID-19 fear.

## Data

Throughout this work, we relied on two sources of COVID-19 data: official surveillance data from the COVID-19 Data Hub (Guidotti and Ardia 2020; Guidotti 2022) and survey-based data from the Delphi US CTIS (Delphi Group, CMU 2020), which contains information on demographics, the types of information sources used by individuals, and self-reported levels of fear. All datasets used in this study are open-source and publicly available. Aggregated data from the Delphi US CTIS survey can be accessed as described in the *Availability of materials and data* section.

We primarily used the COVID-19 Data Hub (Guidotti and Ardia 2020; Guidotti 2022) as our source of surveillance data. Specifically, we used daily new fatalities and confirmed cases—computed from cumulative counts—as well as the total U.S. population. These indicators were used to estimate the daily number of official infections via Sybil (Baccegga et al. 2024). Specifically, this data allows us to reconstruct the dynamics of a Susceptible-Infected-Recovered-Deceased-Susceptible (SIRDS) compartmental model with reinfections over the study period. In this model, the infected compartment represents the estimate of the official number of infections (Álvarez et al. 2021; Astley et al. 2021)—we assumed an average recovery time of 14 days to compensate for the lack of recovery data, which are largely unavailable. While the Data Hub provides additional information, such as vaccination rates and hospital statistics, these were not relevant to our study.

Since the spring of 2020, Facebook has collaborated with both Carnegie Mellon University (CMU) and the University of Maryland (UMD) through its Data for Good program (Facebook 2020) to promote large-scale, daily sur-

Question	Possible responses
(D2) What is your age?	(1) 18-34 years, (2) 35-64 years, (3) 65+ years
(D8) What is the highest degree or level of school you have completed?	(1) Lower than high school, (2) High school / Bachelor’s degree, (3) Postgraduate
(I5) In the past 7 days, from which of the following sources have you received news and information about COVID-19?	(1) Doctors, (2) Scientists, (3) CDC, (4) Government, (5) Politicians, (6) Journalists, (7) Family and friends, (8) Religious leaders, (9) None of the above (other sources not listed here).
(G1) How much do you worry about catching COVID-19?	(1) A great deal, (2) A moderate amount, (3) A little, (4) Not at all.

Table 1: Selected questions and responses from the Delphi US CTIS survey, with labels as in the original survey.

veys developed by these institutions (Astley et al. 2021; Fan et al. 2020). The Delphi Group at CMU administers the U.S. COVID-19 Trends and Impact Survey (Delphi Group, CMU 2020)—Delphi US CTIS—, which collects approximately 50,000 responses per day from Facebook users in the United States. This survey includes self-reported information on symptoms, testing, vaccination, behaviors, and other COVID-19-related topics, and was used to estimate prevalence trends across U.S. states, accounting for direct and indirect reporting (Srivastava et al. 2024). Access to the data was obtained through an agreement with CMU, UMD, and Facebook, as described in the *Ethical Declaration* section. The full set of survey questions in the U.S. is available at (Delphi Group, Carnegie Mellon University 2020).

Specifically, we computed daily aggregated information considering questions about age, education, source of information, and infection-induced fear—a summary of the selected questions and their corresponding response options is provided in Table 1. Importantly, these daily aggregates were calculated using the weights provided in the Delphi US CTIS microdata files. These weights were designed to address the differences between Facebook users and the overall US population, as well as to correct for biases associated with non-response (Salomon et al. 2021). For clarity and simplicity, throughout the remainder of the paper, we refer to responses to D2 as *Age*, D8 as *Education*, I5 as *Source*, and G1 as *Fear*. For *Source*, users could select multiple options, whereas for *Age*, *Education*, and *Fear* responses are mutually exclusive. Therefore, we accounted for all possible combinations of the nine response options in *Source*, totaling 256—also comprising the *None of the above* response, which is used in mutual exclusion with all the other possible answers. We will focus on the relationships between *Age*, *Education*, and *Source* with respect to COVID-19–induced *Fear*, employing the notation presented in Table 2.

Our analysis covers the period from May 2021 to June 2022 across all U.S. states, which combines online activity with self-reported information. While these data sources are inherently biased toward individuals with consistent internet access—specifically on active Facebook users—and may underrepresent certain socio-demographic groups or regions with limited connectivity, these biases are less pronounced in U.S. states where internet access is widespread—hence, offering valuable insights into broader behavioral trends.

**Normalization.** This step primarily facilitates the later examination of correlations and comparisons among variables. By grouping respondents based on *Age*, *Education*, or not grouping at all—denoted by variable  $v$ —, it is straight-

Symbol	Description
$\mathcal{S}$	Set of 256 combinations of <i>Source</i> <sup>1</sup>
$s'$	Singleton information sources from $\mathcal{S}$ , e.g., $\{\text{Doctors}\}$ and $\{\text{Scientists}\}$
$\mathcal{F}$	Set of self-reported fear levels $f \in \mathcal{F}$ , where $\mathcal{F} = \{1, 2, 3, 4\}$
$\sigma_s$	Average number of respondents selecting the combination $s \in \mathcal{S}$
$\sigma_{s'}$	Average number of respondents selecting singleton $s' \in \mathcal{S}$
$\varphi_{s, f}$	Average number of respondents who self-reported a fear level $f \in \mathcal{F}$ , selecting the combination $s \in \mathcal{S}$
$\varphi_s$	Average fear score among respondents selecting the combination $s \in \mathcal{S}$
$\hat{\varphi}_{s'}$	Estimate of average fear score for singletons $s' \in \mathcal{S}$
$v$	Demographic grouping: <i>Age</i> , <i>Education</i> , or no grouping
$t$	Time variable $t \in [1, T]$ , where $T$ denotes the length of the time series, with one observation per day

Table 2: Notation used in the paper.

forward to derive the normalized quantities  $\hat{\sigma}_s$ :

$$\hat{\sigma}_s(v) = \frac{\sigma_s(v)}{\sum_{i \in \mathcal{S}} \sigma_i(v)}, \quad (1)$$

where we dropped the time dependence for ease of notation. Similarly, we define the normalized *Fear* measure  $\hat{\varphi}_{s, f}$  for different levels of self-reported fear, applying an analogous procedure.

**Singleton information sources.** Data on information usage is provided in aggregated form, where each  $s \in \mathcal{S}$  represents a possible combination of the considered information sources. However, to investigate the utilization of individual sources, we extrapolate the proportion of respondents using each singleton information source. Specifically, the average number of people using a specific singleton source  $\hat{\sigma}_{s'}$  is given by

$$\hat{\sigma}_{s'}(v) = \sum_{\forall u \in \mathcal{S}: s' \in u} \hat{\sigma}_u(v), \quad (2)$$

where  $s'$  are the singletons information sources from  $\mathcal{S}$ . Please note that, although  $\hat{\sigma}_{s'}$  is computed starting from the normalized variable  $\hat{\sigma}_s$ , the sum of  $\hat{\sigma}_{s'}$  over all singletons  $s'$  might exceed 1 since individual values of  $\hat{\sigma}_u$  are counted once for each  $s' \in u$ .

**Fear score.** By assigning weights  $w_f$  to each fear level, we define the fear score as

$$\hat{\varphi}_s(v) = \sum_{f \in \mathcal{F}} w_f \cdot \hat{\varphi}_{s, f}(v), \quad (3)$$

where  $w_f \in \{1, 0.34, -0.34, -1\}$ . This formulation ensures that responses such as *A great deal* are counterbal-

<sup>1</sup>In detail,  $\mathcal{S} = \{\{\text{Doctors}\}, \{\text{Scientists}\}, \{\text{CDC}\}, \dots, \{\text{None of the above}\}, \{\text{Doctors, Scientists}\}, \{\text{Doctors, CDC}\}, \dots\}$  is a set containing 256 subsets.

anced by *Not at all*, with a similar compensatory relationship between *A moderate amount* and *A little*.

**Fear score of singleton information sources.** In case of *Fear*, we cannot directly apply the approach used in Equation 2 to obtain the average fear score from singleton source responses. This limitation arises because, for each  $s \in \mathcal{S}$ , the distribution of *Fear* across the selected sources is unknown. For example,  $s = \{CDC, Politicians, Journalists\}$  denotes the average fear score across all U.S. states among respondents who selected *CDC*, *Politicians*, and *Journalists* as their information sources. However, this aggregated value does not reveal how much each source contributes to the self-reported fear—this could be primarily driven by *Journalists*, equally influenced by all three sources, or dominated by a different source within the combination.

To address this, and estimate  $\phi_{s'}$ , we employ linear models to disentangle the contribution of each source to the overall average fear score as

$$\min_{w_{s'|s}} \sum_{t \in T} \left( \hat{\phi}_s(v, t) - \sum_{s' \in s} w_{s'|s} \cdot \hat{\phi}_{s'}(v, t) \right)^2, \quad (4)$$

where  $w_{s'|s}$  represents time-independent weights assigned to each singleton source  $s'$  in the combination  $s$ —this optimization problem is solved for each  $s \in \mathcal{S}$ . These weights are estimated by minimizing the squared difference between the observed average fear score of the combination  $s$ , denoted  $\hat{\phi}_s(v, t)$ , and the weighted sum of the average fear scores of its singleton sources,  $\hat{\phi}_{s'}(v, t)$ . Specifically, we use  $\hat{\phi}_{s'}(v, t)$ —the fear score among respondents who selected  $s'$ —as a proxy to estimate the weights. In this way, for each  $\hat{\phi}_s(v)$ , we determine the contribution of each singleton  $s' \in s$ . Using these weights, we then compute  $\phi_{s'}$  as

$$\phi_{s'}(v) = \sum_{s \in \mathcal{S}} w_{s'|s} \cdot \hat{\phi}_{s'}(v) \quad (5)$$

Only weights from models with statistically significant coefficients—determined via F-tests—are retained to ensure robust attribution.

## Methods

This section describes the primary methodology used in our study, as illustrated in Figure 1.

**Statistical analysis on fear.** Using U.S. data, we assess how different information sources affect COVID-19-related fear through statistical tests—Shapiro–Wilk (Shapiro and Wilk 1965), Kolmogorov–Smirnov (Massey Jr 1951) and Mann–Whitney U (Nachar et al. 2008) tests—and Spearman correlation analyses (Spearman 1961). We further examine how demographic factors—specifically age and education—shape emotional responses, thereby revealing distinct patterns across population groups. Specifically, the Shapiro–Wilk test was used to assess whether a distribution follows normality, whereas the Kolmogorov–Smirnov test was applied to compare two distributions, evaluating differences across their full range, including shape, dispersion, and central tendency. In contrast, the Mann–Whitney U test was employed to detect differences in central tendency between two distributions. The Spearman correlation coefficient was used to quantify the strength and direction of

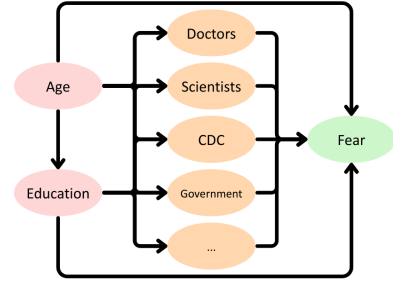


Figure 2: Causal inference model used.

monotonic relationships, allowing us to examine how fear levels co-vary with different information sources.

**Causal inference.** Using causal inference, we evaluate the relative contributions of age, education, and information source to COVID-19-related fear, finding that information source is the most influential factor. In particular, causal inference aims to uncover cause-and-effect relationships rather than mere statistical associations. It employs a range of statistical methods and study designs—such as randomized controlled trials and quasi-experimental approaches—to estimate the effect of an exposure or intervention on an outcome while accounting for potential confounders. Randomized controlled trials remain the gold standard for establishing causality, as randomization helps balance confounding factors across groups. However, these trials are often infeasible or ethically problematic. In such cases, causal inference methods can be applied to observational data, provided key assumptions hold—consistency, positivity, and exchangeability. Moreover, we estimate the average treatment effect (ATE) of different information sources, where the ATE—one of the primary metrics in causal inference—quantifies the expected difference in outcomes between a control treatment (in our case, *None of the above*) and each alternative information source, thereby reflecting the causal impact of the intervention at the population level.

To define the causal inference model—shown in Figure 2—, we use the DoWhy package (Sharma and Kiciman 2020; Blöbaum et al. 2024), a Python library that integrates graphical causal models with statistical methods to specify assumptions, identify estimands, estimate causal effects, and perform robustness checks, including refutation tests. DoWhy was mainly used to estimate the strength of causal relationships (arrow strengths) by fitting a Probabilistic Causal Model (PCM) to the data. For effect estimation, however, we used Ordinary Least Squares (OLS) regression models, adjusting for confounders (*Age* and *Education*) identified in the causal graph, to obtain ATE estimates. DoWhy’s refutation API was applied to validate model robustness through tests like placebo treatments and subset analyses, ensuring the reliability and interpretability of our OLS-based causal estimates from observational data.

In detail, the positivity assumption was verified by confirming that all information sources appear across all *Age* and *Education* strata, ensuring each source has a positive probability of selection. Each source was treated as a binary treatment (selected or not on a given date), assuming consis-

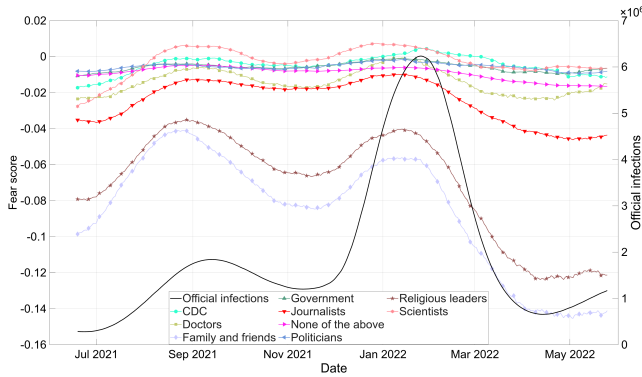


Figure 3: Temporal evolution of  $\phi_{s'}$  for each of the nine singleton information sources—values on the left axis—, alongside the official infection counts in the U.S.—values on the right axis—between May 2021 and June 2022. To reduce noise, official infections and  $\phi_{s'}$  were smoothed using a two-month rolling average.

tent definitions, no meaningful heterogeneity in usage, and additive effects. While the intensity and context of source use may vary (e.g., passive exposure vs. active seeking), such distinctions are not captured in the survey. The analysis further assumes that age and education suffice to control for confounding, though unmeasured factors—such as political ideology, institutional trust, socioeconomic status, and personal traits—may influence results. Consequently, estimated causal effects reflect associations conditional on measured confounders, and causal interpretation relies on the unverifiable assumption of no relevant unmeasured confounding. Sensitivity analyses for unmeasured confounding are beyond the scope of this study.

**Geographical distribution of sources.** Finally, we statistically assess how people use different information sources using the previously described tests and Spearman correlation analyses, while also examining how demographic factors influence information source usage, thereby revealing distinct patterns across population groups. Next, we apply K-means (Hartigan, Wong et al. 1979), spectral (Ng, Jordan, and Weiss 2001), and hierarchical clustering (Johnson 1967) to group U.S. states based on their residents’ reliance on different types of information. Remarkably, the resulting clusters exhibit a strong alignment with state-level political orientation—specifically, whether a state tends to lean Democratic or Republican. In detail, K-means partitions data into  $k$  clusters by iteratively assigning points to the nearest centroid, while spectral clustering uses graph Laplacian eigenvectors to capture non-convex structures before applying a partitioning method such as K-means. Hierarchical clustering builds a dendrogram through agglomerative or divisive steps, allowing flexible cluster counts but at a higher computational cost. Cluster quality is commonly assessed using the Silhouette score, which quantifies how well points fit within their assigned clusters.

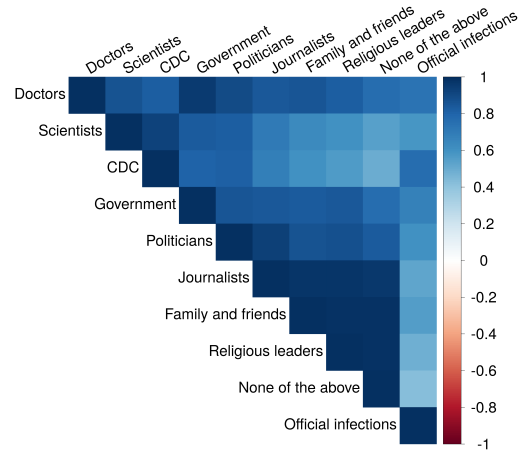


Figure 4: Spearman correlation coefficients among the time series shown in Figure 3.

## Results

**Statistical analysis on fear.** Employing the definitions introduced in the *Data* section, we investigate the drivers behind the evolution of the nationwide U.S. fear score  $\phi_{s'}$ . As a starting point, we examine whether *Fear* differs across the various information sources. In particular, considering the nine distributions derived from the singleton information sources  $s'$ , we first applied the Shapiro–Wilk test, which indicated that none of the distributions are normally distributed. Next, to assess whether these distributions differ significantly—both within groups (across the nine singleton information sources for each *Age* or *Education* group and at the population level) and between groups (across different *Age* or *Education* groups)—we applied the Kolmogorov–Smirnov and Mann–Whitney U tests. The consistently significant results indicate meaningful variation in fear-score distributions at both levels, reflecting demographic and informational heterogeneity.

In light of these findings, Figure 3 presents the temporal evolution of the singleton fear scores  $\phi_{s'}$ , alongside the official number of infections across the U.S. Notably, *Religious leaders* and *Family and friends* emerge as significant outliers, consistently associated with lower fear scores<sup>2</sup>. Moreover, the fear score  $\phi_{s'}$  closely mirrors fluctuations in official infection numbers, indicating a strong correlation between the two—as shown in Figure 4, where we can notice that  $\phi_{s'}$  is more sensitive to relative increases in case numbers than to absolute levels.

Some sources show even greater sensitivity. The coefficient of variation<sup>3</sup> is particularly high for *Scientists* ( $\approx 3$ ) and the *CDC* ( $\approx 1$ ), whereas all other sources remain below 0.5, indicating moderate variability. This pattern illustrates how fear intensifies with the rising visibility of COVID-19 cases, dominating public discourse. The moderate to high

<sup>2</sup>Fear score spanning values around zero reflects design choice of assigning weights that counterbalance the associated responses in the survey, as defined in Equation 3.

<sup>3</sup>The coefficient of variation is the standard deviation divided by the mean’s absolute value, measuring relative variability.

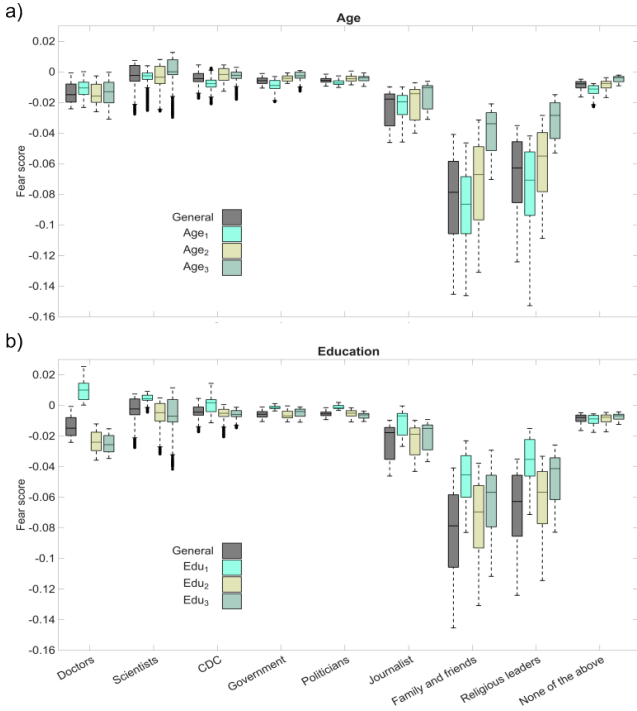


Figure 5: Boxplots showing the distribution of  $\phi_{s'}$  across the nine singleton information sources, stratified by *a)* *Age*—where *Age*<sub>1</sub>, *Age*<sub>2</sub>, and *Age*<sub>3</sub> refers to the three *Age* groups—and *b)* *Education* groups—where *Edu*<sub>1</sub>, *Edu*<sub>2</sub>, and *Edu*<sub>3</sub> refers to the three *Education* groups.

variation highlights its strong dependence on fluctuations in official case numbers.

Among all sources, *Family and friends* and *Journalists* slightly anticipate phase transitions in infection trends: their signal  $\phi_{s'}$  precedes both the initial rise and the peak decline during the Delta and Omicron waves (Dattani and Rodés-Guirao 2024). This pattern may reflect an anticipatory response driven by early information or heightened awareness within these social and media networks.

In addition, singleton fear scores exhibit strong mutual correlations, as demonstrated by the Spearman correlation coefficients in Figure 4. A strong correlation among the fear-related time series indicates that, regardless of the specific source of information, the perceived fear tends to vary consistently across sources. A lower correlation is observed for the two outliers mentioned above, as well as for *None of the above*, which exhibits a flatter trend. However, these three time series are highly correlated with one another and with *Journalists*, indicating that individuals relying on personal or alternative information sources may develop perceptions of fear that differ from those shaped by institutional or official sources. This may point to the existence of an alternative information ecosystem—insulated from broader media trends—where emotional responses are shaped by interpersonal communication or internal beliefs rather than external news flows.

Finally, Figure 5 displays boxplots illustrating the distribution of the signal  $\phi_{s'}$  across the nine singleton information sources, stratified by *Age* and *Education* groups. By exclud-

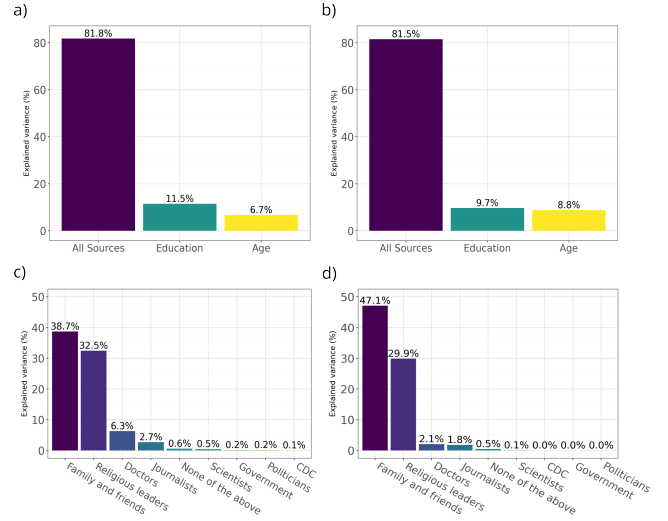


Figure 6: Estimated direct effects on *Fear*. Panels *a)* and *b)* show variance explained by each variable in the first and second waves, respectively. Panels *c)* and *d)* show the influence of each information source.

ing the temporal dimension, these distributions offer a concise statistical summary of how fear scores vary across different age and education strata. Additionally, it includes the overall distribution without stratification by *Age* or *Education*—note that the overall boxplot is not merely the average of the stratified ones, as the estimates of  $\phi_{s'}$  were obtained using separate linear models for each grouping variable, as detailed in Equation 5. Specifically, focusing on *Age*,  $\phi_{s'}$  increases with age, with *Age*<sub>1</sub> exhibiting the lowest fear score and *Age*<sub>3</sub> the highest, across almost all sources—a few exceptions to this trend are observed for *CDC*, *Doctors*, and *Scientists*, where the pattern differs slightly. When focusing on *Education*,  $\phi_{s'}$  generally decreases from *Edu*<sub>1</sub> to *Edu*<sub>2</sub>, and in most cases rises again with *Edu*<sub>3</sub>, although in some instances it continues to decline. This behavior highlights the nuanced effect of education on perceived fear, suggesting that while higher education may generally be associated with greater awareness and concern, its influence can vary depending on the source of information and potentially other demographic or contextual factors. In addition, *Religious leaders* and *Family and friends* continue to stand out as outliers in the distribution.

**Causal inference.** The findings from the previous section indicate that  $\phi_{s'}$  varies significantly not only with the sources of information people rely on but also with their age and education. Nonetheless, identifying the primary driver of perceived fear remains challenging. Therefore, we employ causal inference methods to investigate these factors and determine which variable among *Source*, *Age*, and *Education* has the strongest influence on *Fear*.

Figure 2 illustrates the causal inference model, featuring nine binary *Source* variables (one-hot encoded from the original categorical source), continuous outcome *Fear*, and categorical confounders *Age*, *Education*  $\in \{1, 2, 3\}$ . Direct effects flow from each *Source*  $\rightarrow$  *Fear* and demographics *Age*, *Education*  $\rightarrow$  *Fear*. Critical confounding arises via

Source	ATE		Source	ATE	
	W1	W2		W1	W2
Scientists	0.24	0.37	Doctors	-0.17	0.00
Government	0.18	0.25	Journalists	-0.38	-0.25
CDC	0.18	0.33	Religious leaders	-1.62	-1.50
Politicians	0.14	0.24	Family and friends	-1.90	-1.89

Table 3: ATE of information sources on *Fear* across two waves using *None of the above* as the “control” source. W1 and W2 denote the first and second waves of the data.

*Age, Education*  $\rightarrow$  *Source*, where demographics determine information source exposure, biasing naive source-fear associations; additionally, *Age*  $\rightarrow$  *Education* captures age’s effect on education. This DAG structure necessitates adjustment for both confounders to identify the causal effects of information sources on fear. We exclude infection counts in the model because we assume that individuals learn about epidemiological conditions exclusively through information sources. In the absence of such sources, individuals would have no access to the actual infection counts. To account for temporal dynamics, we analyze two distinct waves, separated by the date on which infections reached their minimum between the two periods under consideration: May 2021–November 11, 2021, and November 12, 2021–June 2022. Within each wave-specific analysis, we acknowledge that daily observations may exhibit temporal correlation.

Specifically, we applied this model—normalizing  $\phi_{s'}$ —to estimate the strength of each direct causal pathway leading to *Fear*. Our analysis shows that *Source* is the most influential variable, accounting for 81.8% of the normalized  $\phi_{s'}$  variance in the first wave and 81.5% in the second—Figures 6.a) and 6.b). This indicates that this variable plays a dominant role in shaping fear responses within the population studied. In comparison, demographic factors such as *Age* and *Education* contribute more modestly, accounting for 6.7%–8.8% and 11.5%–9.7% of the variance, respectively, across the two waves. These findings suggest that while individual characteristics do have some impact, the *Source* variable is the primary driver. Moreover, Figures 6.c) and 6.d) show the influence of each *Source*, with *Family and friends* and *Religious leaders* exerting the greatest influence, while all others have smaller effects—except for *Doctors* in the first wave, which account for 6.3%.

Finally, we estimate the ATE of different information sources on *Fear*, using *None of the above* as the “control” source. Table 3 presents the results. In both waves, the ranking of sources in decreasing order is largely consistent, with the exception of *CDC* in the second wave, whose effect is higher and closer to that of *Scientists*. Interestingly, from the first to the second wave, the ATE of each source increases, indicating that during the Omicron wave, people were more afraid when using a source other than the “control” source. Notably, we observe that people are less afraid when obtaining information from the two outliers, *Family and friends* and *Religious leaders*, as well as from *Journalists*, suggesting lower trust in these sources, whereas they are more afraid when obtaining information from more official sources such as *Scientists*, *Government*, *CDC*, and *Politicians*.

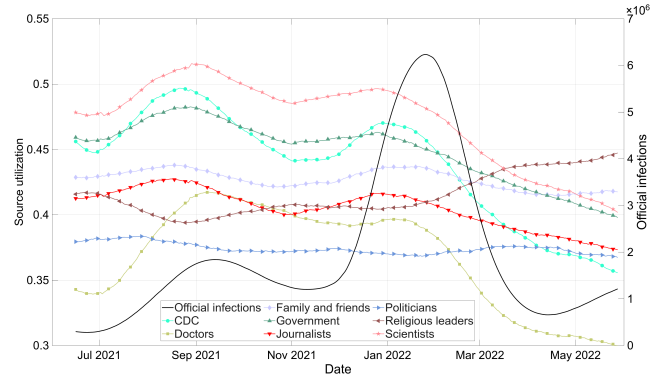


Figure 7: Temporal evolution of  $\hat{\sigma}_{s'}$  for each of the nine singleton information sources—values on the left axis—, alongside the official infection counts in the U.S.—values on the right axis—between May 2021 and June 2022. We chose not to display *None of the above* as its values are consistently near zero and exhibit minimal variation.

### Geographical distribution of sources: U.S. nationwide.

Using the definitions introduced in the *Data* section, we analyze patterns in the use of each singleton information source, independently of *Fear*, represented by  $\hat{\sigma}_{s'}$ . As before, we begin by analyzing the nine distributions: the Shapiro–Wilk test indicates that none follow a normal distribution. To assess differences—both within and between groups—we used the Kolmogorov–Smirnov and Mann–Whitney U tests. The observed significant differences reinforce the idea that perceived uncertainty varies meaningfully across demographic segments and source groupings.

Based on this evidence, Figure 7 shows the evolution of the fraction of respondents relying on each information source, alongside the official number of infections across the U.S. It is notable that *None of the above* consistently shows values near zero with little variation, and is therefore excluded from the visualization, indicating that few respondents rely on sources outside those listed. Similar to the fear score, respondents’ reliance on information sources closely follows infection trends, showing strong correlation and greater sensitivity to relative increases in cases, except for *Politicians*, whose pattern remains largely flat and uncorrelated—Figure 8. Some sources exhibit moderate sensitivity. The coefficient of variation varies between approximately 0.25 for *None of the above* to around 0.1 for *Doctors* and *CDC*, and is lower for other sources, indicating moderate to low variability.

Respondents’ use of information sources displays strong mutual correlations, as shown in Figure 8, which presents the Spearman correlation coefficients. Within this context, three sources emerge as outliers: *Religious leaders*—as previously noted—, *None of the above*, and *Politicians*. Specifically, *Religious leaders* and *None of the above* display negative correlations with all other time series and a positive correlation with each other. This pattern suggests that their trends move in the opposite direction relative to the other sources, indicating that as infection rises, individuals tend to shift away from these less conventional or less trusted

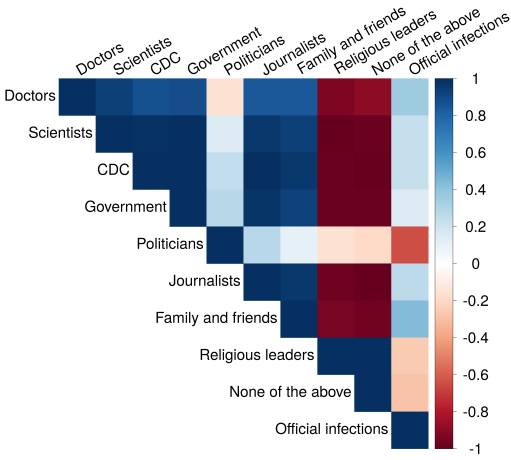


Figure 8: Spearman correlation coefficients among the time series shown in Figure 7.

sources toward more reliable information channels—an inference supported by their negative correlation with official infection numbers. In contrast, *Politicians* exhibit negative correlations with *Religious leaders*, *None of the above*, and *Doctors*, while showing a small positive correlation with the other sources. As illustrated in Figure 7, the time series for *Politicians* remains relatively flat, implying that public reliance on political figures as information providers remains largely stable over time, despite fluctuations in infection severity.

Finally, Figure 9 displays boxplots illustrating the distribution of the fraction of individuals relying on each singleton information source, stratified by *Age* and *Education* groups, alongside the overall distribution aggregated without stratification. In this case as well, we excluded *None of the above* from the visualization, as it stands out as a clear outlier in both instances. Three clear patterns emerge when moving from *Age*<sub>1</sub> to *Age*<sub>3</sub> and from *Edu*<sub>1</sub> to *Edu*<sub>3</sub>. First, certain sources maintain a relatively stable or flat level of reliance across these groups, suggesting that demographic factors have little effect on their usage—like *Family and friends*, *Politicians*, and *None of the above*. Second, *Religious leaders* exhibit a decreasing trend, with younger or less educated groups relying on them more than older or more educated ones. Third, the remaining sources—institutional or expert ones—show increased reliance as *Age* and *Education* rise—meaning older or more educated individuals tend to trust these sources more.

**Geographical distribution of sources: U.S. states.** To further understand patterns in the use of information sources, we conduct a geographical analysis across U.S. states. The United States presents a diverse socio-economic landscape, with substantial variation in income levels, educational attainment, and cultural norms across regions. These differences are likely to influence how individuals seek and trust information, particularly in the context of a public health crisis such as the COVID-19 pandemic. By examining the spatial distribution of preferred information sources, we aim to uncover regional trends and disparities that may reflect un-

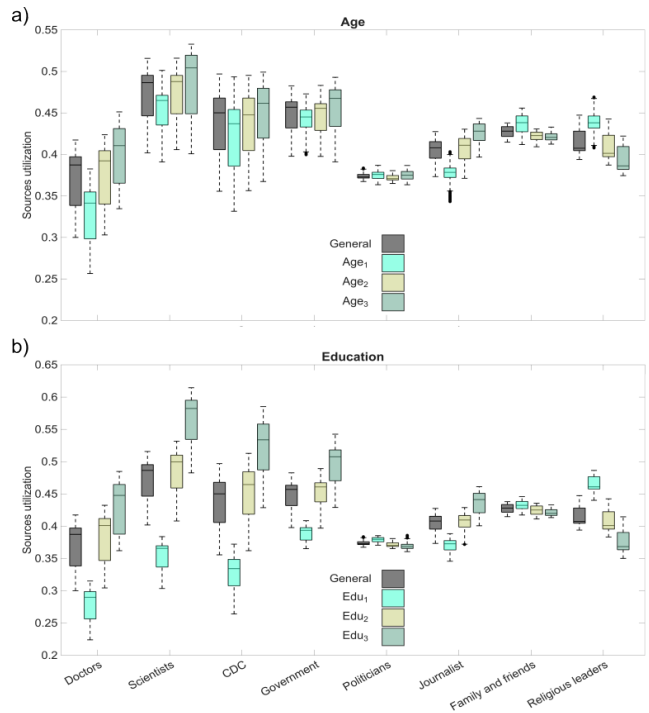


Figure 9: Boxplots showing the distribution of the fraction of respondents relying on each information source, stratified by a) *Age*—where *Age*<sub>1</sub>, *Age*<sub>2</sub>, and *Age*<sub>3</sub> refers to the three *Age* groups—and b) *Education* groups—where *Edu*<sub>1</sub>, *Edu*<sub>2</sub>, and *Edu*<sub>3</sub> refers to the three *Education* groups. We chose not to display *None of the above* as its values are consistently near zero and exhibit minimal variation.

derlying socio-demographic and economic characteristics. Hence, for each U.S. state, we compute the average reliance on each singleton information source—from  $\hat{\sigma}_s$ —, without stratification by *Age* or *Education*, resulting in nine values per state. These averages are then used to cluster the states using K-means, spectral, and hierarchical clustering methods.

Based on the Silhouette score, we determined that two clusters provide the optimal partitioning. Figure 10 illustrates the resulting clusters, with each state colored according to its assigned cluster. Interestingly, by chance, we obtained two clusters that correspond closely to the two major U.S. political affiliations: Democratic and Republican. Specifically, Figure 10.a) compares the derived clusters to the 2020 U.S. political elections results, while Figure 10.b) shows the comparison with the 2024 elections outcomes, both obtained using K-means clustering—similar results were obtained with hierarchical and spectral clustering. States that were misclassified—i.e., assigned to the cluster contrary to their political affiliation in the given year—are marked with a grid overlay in the contrasting cluster color. We observe that only three states were assigned to the opposite cluster in the 2020 elections, while five states were assigned to the opposite cluster in the 2024 elections. Interestingly, these states—except for Alaska—are swing states between the 2020 and 2024 political elections, which makes them inherently more difficult to classify. These re-

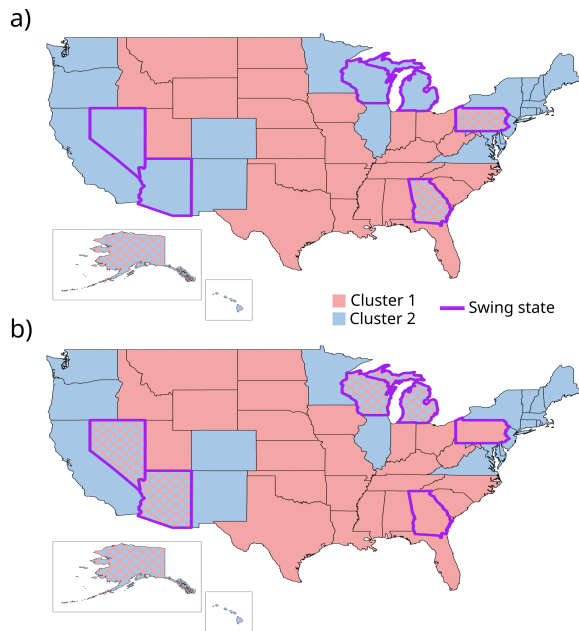


Figure 10: Clusters derived from K-means analysis based on average reliance on each information source,  $\hat{\sigma}_{s'}$ , across U.S. states, without stratifying by *Age* or *Education*. These clusters are compared with the results of the a) 2020 and b) 2024 U.S. political elections. Misclassified states are overlaid with a contrasting grid. States with a purple border indicate swing states between the 2020 and 2024 U.S. political elections.

sults suggest that the clustering based on information source reliance closely reflects established political divisions, with misclassifications primarily occurring in politically competitive swing states. This underscores the sensitivity of information consumption patterns to shifting political landscapes.

## Conclusion

Building on behavioral and demographic data, this study explores the factors driving fear of COVID-19 infection, focusing on how information sources and demographics shape emotional responses. We examine how channels such as social media, traditional journalism, government briefings, and interpersonal communication relate to differences in perceived fear across the U.S., analyzing data from May 2021 to June 2022, covering the Delta and Omicron waves.

Recognizing potential biases in digital platforms, particularly toward users with consistent internet access, we contextualize our findings within the socio-economic and geographic diversity of the U.S. Regional disparities in media habits, internet penetration, and education underscore the importance of a geographically nuanced approach to understanding information dynamics and public emotion. Moreover, this study analyzes data exclusively from the U.S. Delphi CTIS survey, which is restricted to American respondents. While this enables detailed causal inference within the U.S. context, the work could be extended to other countries if comparable longitudinal panel data on COVID-19 fear, in-

formation sources, and related behaviors become available in the future.

Our analysis shows that COVID-19-related fear associated with the considered information sources is strongly correlated across sources and with the number of confirmed infections. Using causal inference techniques, we quantified the effects of age, education, and information sources on perceived fear. Information sources emerged as the most significant driver, while demographics also shape emotional reactions and preferences for specific types of information, revealing distinct behavioral patterns across age and education groups. These results underscore the pivotal role of the information environment in shaping public fear during health crises. The credibility, framing, and volume of content can amplify or mitigate fear, with misinformation posing a serious threat to risk perception and trust. Ensuring access to verified, reliable sources is therefore critical for informed decision-making and emotional resilience.

Moreover, our findings reveal a strong connection between information ecosystems and political behavior. Clustering analysis showed that patterns of reliance on specific information sources across U.S. states closely aligned with political orientations during the 2020 and 2024 election cycles. These results underscore the broader societal impact of informational environments, demonstrating their influence not only on emotional responses but also on civic attitudes and decision-making. In this context, it becomes imperative that official information channels maintain the highest standards of accuracy and credibility. The dissemination of misinformation—whether intentional or due to negligence—by institutional sources not only distorts public understanding but also undermines democratic processes by shaping political beliefs on falsehoods. Therefore, safeguarding trusted information sources from distortion is crucial for protecting both public health and the integrity of democratic society.

## References

- Álvarez, J.; et al. 2021. Estimating active cases of COVID-19. *MedRxiv*, 2021–12.
- Astley, C. M.; et al. 2021. Global monitoring of the impact of the COVID-19 pandemic through online surveys sampled from the Facebook user base. *Proceedings of the National Academy of Sciences*, 118(51): e2111455118.
- Baccega, D.; Castagno, P.; Fernández Anta, A.; and Sereno, M. 2024. Enhancing COVID-19 forecasting precision through the integration of compartmental models, machine learning and variants. *Scientific Reports*, 14(1): 19220.
- Bernardin, A.; and Perez-Acle, T. 2025. Assessing the impact of misinformation during the spread of infectious diseases. *Scientific Reports*, 15(1): 34740.
- Blöbaum, P.; et al. 2024. DoWhy-GCM: An Extension of DoWhy for Causal Inference in Graphical Causal Models. *Journal of Machine Learning Research*, 25(147): 1–7.
- Caceres, M. M. F.; et al. 2022. The impact of misinformation on the COVID-19 pandemic. *AIMS public health*, 9(2): 262.

- Chai, Y.; et al. 2022. Measuring daily-life fear perception change: A computational study in the context of COVID-19. *Plos one*, 17(12): e0278322.
- Cinelli, M.; et al. 2020. The COVID-19 social media infodemic. *Scientific reports*, 10(1): 16598.
- Coelho, C. M.; Suttiwan, P.; Arato, N.; and Zsido, A. N. 2020. On the nature of fear and anxiety triggered by COVID-19. *Frontiers in psychology*, 11: 581314.
- Dattani, S.; and Rodés-Guirao, L. 2024. 17 Key Charts to Understand the COVID-19 Pandemic. *Our World in Data*. Accessed: 2025-07-28.
- Delphi Group, Carnegie Mellon University. 2020. Delphi's COVID-19 Trends and Impact Survey (CTIS). <https://delphi.cmu.edu/epidemic-signals/ctis/>. Accessed: 2025-07-28.
- Delphi Group, CMU. 2020. COVIDcast. <https://delphi.cmu.edu/covidcast/>. Accessed: 2025-07-28.
- Doshi, D.; et al. 2021. Assessing coronavirus fear in Indian population using the fear of COVID-19 scale. *International journal of mental health and addiction*, 19(6): 2383–2391.
- Eder, S. J.; et al. 2021. Predicting fear and perceived health during the COVID-19 pandemic using machine learning: A cross-national longitudinal study. *Plos one*, 16(3): e0247997.
- Entradas, M. 2022. In science we trust: The effects of information sources on COVID-19 risk perceptions. *Health Communication*, 37(14): 1715–1723.
- Facebook. 2020. Facebook Data for Good: COVID-19 Symptom Survey – Request for Data Access.
- Fan, J.; et al. 2020. The University of Maryland Social Data Science Center Global COVID-19 Trends and Impact Survey. *Partnership with Facebook*.
- Guidotti, E. 2022. A worldwide epidemiological database for COVID-19 at fine-grained spatial resolution. *Scientific Data*, 9(1): 112.
- Guidotti, E.; and Ardia, D. 2020. COVID-19 Data Hub. *Journal of Open Source Software*, 5(51): 2376.
- Habib, H.; and Nithyanand, R. 2023. The Morbid Realities of Social Media: An Investigation into the Narratives Shared by the Deceased Victims of COVID-19. In *Proceedings of the International AAAI Conference on Web and Social Media*, volume 17, 303–314.
- Hartigan, J. A.; Wong, M. A.; et al. 1979. A k-means clustering algorithm. *Applied statistics*, 28(1): 100–108.
- Johnson, S. C. 1967. Hierarchical clustering schemes. *Psychometrika*, 32(3): 241–254.
- Jones, R.; Mougouei, D.; and Evans, S. L. 2021. Understanding the emotional response to Covid-19 information in news and social media: A mental health perspective. *Human behavior and emerging technologies*, 3(5): 832–842.
- Li, R. 2022. Fear of COVID-19: What causes fear and how individuals cope with it. *Health Communication*, 37(13): 1563–1572.
- Loomba, S.; et al. 2021. Measuring the impact of COVID-19 vaccine misinformation on vaccination intent in the UK and USA. *Nature human behaviour*, 5(3): 337–348.
- Lu, L.; et al. 2021. Source trust and COVID-19 information sharing: the mediating roles of emotions and beliefs about sharing. *Health Education & Behavior*, 48(2): 132–139.
- Massey Jr, F. J. 1951. The Kolmogorov-Smirnov test for goodness of fit. *Journal of the American statistical Association*, 46(253): 68–78.
- Mertens, G.; Lodder, P.; Smeets, T.; and Duijndam, S. 2022. Fear of COVID-19 predicts vaccination willingness 14 months later. *Journal of anxiety disorders*, 88: 102574.
- Miyazaki, K.; et al. 2023. "This is fake news": Characterizing the spontaneous debunking from twitter users to COVID-19 false information. In *Proc. of the International AAAI Conference on Web and Social Media*, volume 17, 650–661.
- Nachar, N.; et al. 2008. The Mann-Whitney U: A test for assessing whether two independent samples come from the same distribution. *Tutorials in quantitative Methods for Psychology*, 4(1): 13–20.
- Ng, A.; Jordan, M.; and Weiss, Y. 2001. On Spectral Clustering: Analysis and an algorithm. In Dietterich, T.; Becker, S.; and Ghahramani, Z., eds., *Advances in Neural Information Processing Systems*, volume 14. MIT Press.
- Nino, M.; Harris, C.; Drawve, G.; and Fitzpatrick, K. M. 2021. Race and ethnicity, gender, and age on perceived threats and fear of COVID-19: Evidence from two national data sources. *SSM-population health*, 13: 100717.
- Oliveira, F. B.; et al. 2023. Beyond fear and anger: A global analysis of emotional response to COVID-19 news on twitter. *Online Social Networks and Media*, 36: 100253.
- Reisdorf, B.; et al. 2021. Information seeking patterns and COVID-19 in the United States. *Journal of Quantitative Description: Digital Media*, 1.
- Retzlaff, C. O.; et al. 2022. Fear, behaviour, and the COVID-19 pandemic: a city-scale agent-based model using socio-demographic and spatial map data. *Journal of Artificial Societies and Social Simulation*, 25(1).
- Salomon, J. A.; et al. 2021. The US COVID-19 Trends and Impact Survey: Continuous real-time measurement of COVID-19 symptoms, risks, protective behaviors, testing, and vaccination. *Proceedings of the National Academy of Sciences*, 118(51): e2111454118.
- Seo, H.; Xiong, A.; Lee, S.; and Lee, D. 2022. If you have a reliable source, say something: effects of correction comments on COVID-19 misinformation. In *Proceedings of the international AAAI conference on web and social media*, volume 16, 896–907.
- Shapiro, S. S.; and Wilk, M. B. 1965. An analysis of variance test for normality (complete samples). *Biometrika*, 52(3-4): 591–611.
- Sharma, A.; and Kiciman, E. 2020. DoWhy: An End-to-End Library for Causal Inference. *arXiv preprint arXiv:2011.04216*.
- Sharma, K.; Zhang, Y.; and Liu, Y. 2022. Covid-19 vaccine misinformation campaigns and social media narratives. In *Proceedings of the International AAAI Conference on Web and social media*, volume 16, 920–931.

Spearman, C. 1961. The proof and measurement of association between two things.

Srivastava, A.; Ramirez, J. M.; Díaz-Aranda, S.; Aguilar, J.; Fernández Anta, A.; Ortega, A.; and Lillo, R. E. 2024. Nowcasting Temporal Trends Using Indirect Surveys. *Proceedings of the AAAI Conference on Artificial Intelligence*, 38(20): 22359–22367.

Van Der Linden, S. 2022. Misinformation: susceptibility, spread, and interventions to immunize the public. *Nature medicine*, 28(3): 460–467.

Weinzierl, M.; Hopfer, S.; and Harabagiu, S. M. 2021. Misinformation adoption or rejection in the era of COVID-19. In *Proceedings of the International AAAI Conference on Web and Social Media*, volume 15, 787–795.

## Checklist

### 1. For most authors...

- (a) Would answering this research question advance science without violating social contracts, such as violating privacy norms, perpetuating unfair profiling, exacerbating the socio-economic divide, or implying disrespect to societies or cultures? **Yes, see the [Data](#) and [Ethical declaration](#) sections.**
- (b) Do your main claims in the abstract and introduction accurately reflect the paper’s contributions and scope? **Yes, the [Abstract](#) and the [Introduction](#) section state the main contributions of the paper, and we explicitly summarize them in a dedicated [Contributions](#) subsection within the [Introduction](#) section.**
- (c) Do you clarify how the proposed methodological approach is appropriate for the claims made? **Yes, in the [Methods](#) section.**
- (d) Do you clarify what are possible artifacts in the data used, given population-specific distributions? **Yes, in the [Data](#) and [Conclusion](#) sections.**
- (e) Did you describe the limitations of your work? **Yes, in the [Data](#), [Methods](#), and [Results](#) sections.**
- (f) Did you discuss any potential negative societal impacts of your work? **NA.**
- (g) Did you discuss any potential misuse of your work? **NA.**
- (h) Did you describe steps taken to prevent or mitigate potential negative outcomes of the research, such as data and model documentation, data anonymization, responsible release, access control, and the reproducibility of findings? **NA.**
- (i) Have you read the ethics review guidelines and ensured that your paper conforms to them? **Yes.**

### 2. Additionally, if your study involves hypotheses testing...

- (a) Did you clearly state the assumptions underlying all theoretical results? **NA**
- (b) Have you provided justifications for all theoretical results? **NA**
- (c) Did you discuss competing hypotheses or theories that might challenge or complement your theoretical results? **NA**

- (d) Have you considered alternative mechanisms or explanations that might account for the same outcomes observed in your study? **NA**
- (e) Did you address potential biases or limitations in your theoretical framework? **NA**
- (f) Have you related your theoretical results to the existing literature in social science? **NA**
- (g) Did you discuss the implications of your theoretical results for policy, practice, or further research in the social science domain? **Yes, in the [Conclusion](#) section.**

### 3. Additionally, if you are including theoretical proofs...

- (a) Did you state the full set of assumptions of all theoretical results? **NA**
- (b) Did you include complete proofs of all theoretical results? **NA**

### 4. Additionally, if you ran machine learning experiments...

- (a) Did you include the code, data, and instructions needed to reproduce the main experimental results (either in the supplemental material or as a URL)? **Yes, see the [Availability of materials and data](#) section.**
- (b) Did you specify all the training details (e.g., data splits, hyperparameters, how they were chosen)? **NA**
- (c) Did you report error bars (e.g., with respect to the random seed after running experiments multiple times)? **NA**
- (d) Did you include the total amount of compute and the type of resources used (e.g., type of GPUs, internal cluster, or cloud provider)? **NA**
- (e) Do you justify how the proposed evaluation is sufficient and appropriate to the claims made? **NA**
- (f) Do you discuss what is “the cost” of misclassification and fault (in)tolerance? **NA**

### 5. Additionally, if you are using existing assets (e.g., code, data, models) or curating/releasing new assets, **without compromising anonymity**...

- (a) If your work uses existing assets, did you cite the creators? **Yes, we have cited relevant papers.**
- (b) Did you mention the license of the assets? **NA**
- (c) Did you include any new assets in the supplemental material or as a URL? **NA**
- (d) Did you discuss whether and how consent was obtained from people whose data you’re using/curating? **Yes, see the [Ethical declaration](#) section.**
- (e) Did you discuss whether the data you are using/curating contains personally identifiable information or offensive content? **Yes, the [data we used does not contain personally identifiable information or offensive content](#).**
- (f) If you are curating or releasing new datasets, did you discuss how you intend to make your datasets FAIR? **NA**
- (g) If you are curating or releasing new datasets, did you create a Datasheet for the Dataset? **NA**

6. Additionally, if you used crowdsourcing or conducted research with human subjects, **without compromising anonymity**...
- (a) Did you include the full text of instructions given to participants and screenshots? *NA*
  - (b) Did you describe any potential participant risks, with mentions of Institutional Review Board (IRB) approvals? *NA*
  - (c) Did you include the estimated hourly wage paid to participants and the total amount spent on participant compensation? *NA*
  - (d) Did you discuss how data is stored, shared, and de-identified? *NA*

## Appendix A: Extended analysis on clustering

In addition to the analysis presented in the *Results* section—specifically in the **Geographical distribution of sources: U.S. states** subsection—we provide additional details on clustering using  $\hat{\sigma}_{s'}$ . We also repeat the analysis with alternative inputs, including  $\phi_{s'}$  alone and in combination with  $\hat{\sigma}_{s'}$ . In each case, we present the clusters obtained using K-means, noting that similar results were obtained with hierarchical and spectral clustering methods.

**Clustering using  $\hat{\sigma}_{s'}$ .** Alongside the results shown in the *Results* section, we incorporate demographic information by computing, for each U.S. state, the average reliance on each singleton information source, grouped by *Age*, resulting in 27 values per state. As shown in Figure 11, this adjustment reduced misclassifications in the 2024 elections, with only Wisconsin and Alaska assigned to the opposite cluster—but it led to a slight increase in misclassifications for the 2020 elections. A similar improvement is observed when combining information source preferences with *Education* levels.

The improved classification performance observed for the 2024 elections when incorporating age and education suggests that these demographic variables became more closely associated with political orientation, likely due to shifts in how different age and education groups access and respond to information. In contrast, the reduced accuracy for the 2020 elections indicates that these factors were less informative during that period, possibly due to more uniform voting patterns across demographics or the influence of external events such as the COVID-19 pandemic.

**Clustering using  $\phi_{s'}$ .** For each U.S. state, we compute the fear score for each singleton information source,  $\phi_{s'}$ , without stratifying by *Age* or *Education*, resulting in nine values per state. Figure 12 presents the resulting clusters and compares them with the outcomes of the 2020 and 2024 political elections.

Compared to the clusters obtained using  $\hat{\sigma}_{s'}$ , a larger number of states are misclassified in both elections—specifically, Colorado, Connecticut, Delaware, Illinois, Maine, Massachusetts, Minnesota, New Hampshire, Oregon, Rhode Island, Texas, Vermont, Virginia, and Washington. Notably, swing states are misclassified only in the 2020 elections, but appear in the correct cluster for 2024. Additionally, Alaska is now correctly classified in both elections.

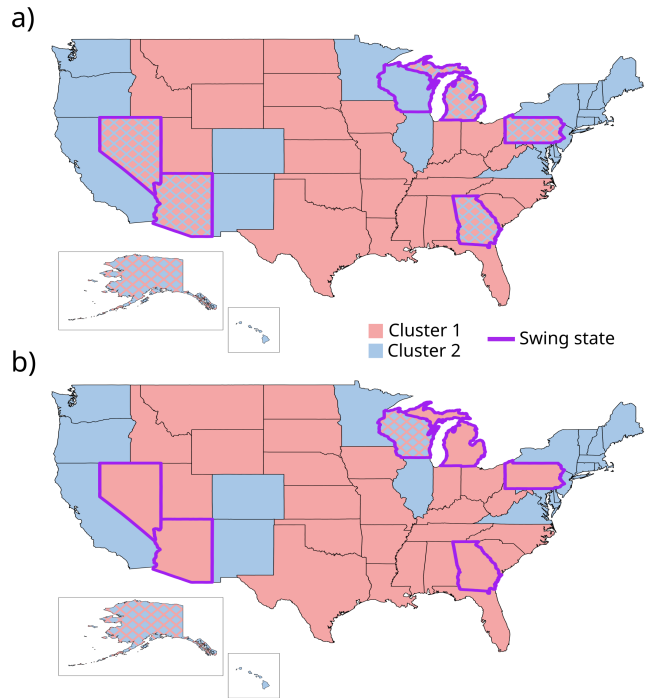


Figure 11: Clusters derived from K-means analysis based on average reliance on each singleton information source,  $\hat{\sigma}_{s'}$ , across U.S. states, stratifying by *Age* or *Education*. These clusters are compared with the results of the a) 2020 and b) 2024 U.S. political elections.

Next, we stratify the data by *Age* and *Education*, yielding 27 values per state. Stratifying by *Age* yields similar results, with the same set of states appearing misclassified. When stratifying by *Education*, two additional states—New York and Maryland—are misclassified in both the 2020 and 2024 elections. This shift suggests that, for these states, educational differences may influence the relationship between fear scores and political alignment in a manner that diverges from the general pattern observed without stratification by education.

More broadly, the presence of traditionally Democratic-leaning states among those misclassified indicates that ideological or cultural factors—such as attitudes toward information sources, regional media ecosystems, or local political discourse—might play a role in shaping fear perception patterns that do not align neatly with national political divisions.

### Clustering using $\hat{\sigma}_{s'}$ and $\phi_{s'}$ .

For each U.S. state, we compute the average reliance  $\hat{\sigma}_{s'}$  and fear scores  $\phi_{s'}$  for each singleton information source without stratifying by *Age* or *Education*, resulting in 18 values per state. Figure 13 presents the resulting clusters obtained and compares them to the outcomes of the 2020 and 2024 U.S. political elections.

When combining both  $\hat{\sigma}_{s'}$  and  $\phi_{s'}$ , we observe that five states—Alaska, Georgia, Michigan, Pennsylvania, and Wisconsin—are misclassified for the 2020 elections, while only three states—Alaska, Arizona, and Nevada—are mis-

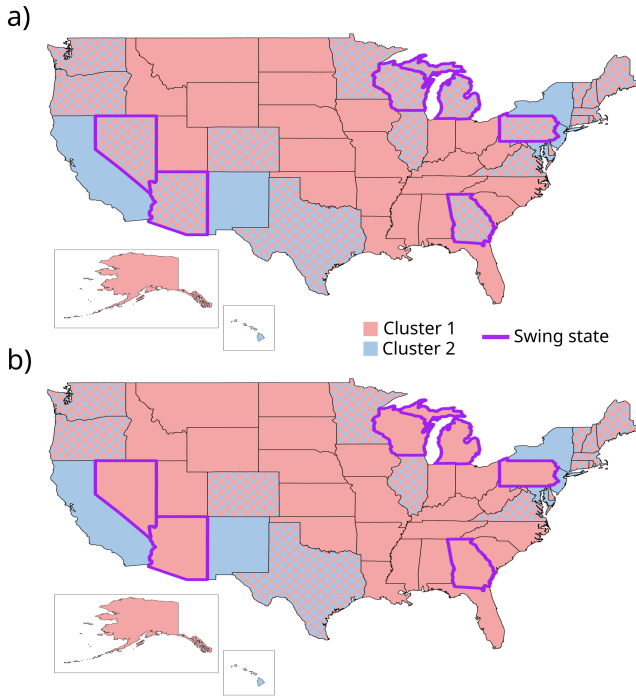


Figure 12: Clusters derived from K-means analysis based on the average respondents' fear score for each singleton information source,  $\phi_{s'}$ , across U.S. states, without stratification by *Age* or *Education*. These clusters are compared with the results of the a) 2020 and b) 2024 U.S. political elections.

classified for the 2024 elections.

Next, we stratify the data separately by *Age* and *Education* for both  $\hat{\sigma}_{s'}$  and  $\phi_{s'}$ , yielding 54 values per state. Stratifying by *Education* yields similar results, with the same set of states appearing misclassified. In contrast, when stratifying by *Age*, only Alaska remains in the wrong cluster for the 2024 elections. This suggests that age-related differences in information consumption and fear perception play a key role in accurately classifying Arizona and Nevada. In these states, incorporating age stratification captures important nuances in how fear and reliance on information sources vary across generations, ultimately aligning their political clustering more accurately.

Interestingly, Wisconsin exhibits the opposite pattern in the 2024 elections. While clustering with  $\hat{\sigma}_{s'}$  and stratifying by age alone is insufficient for correct classification, incorporating fear scores—or a combination of fear and reliance for each information source—is essential for accurate placement. This suggests that, in Wisconsin, the emotional response to information sources plays a more decisive role in shaping political alignment than demographic factors alone.

### Ethical declaration

Further details will be provided upon acceptance, in accordance with double-blinded submission requirements.

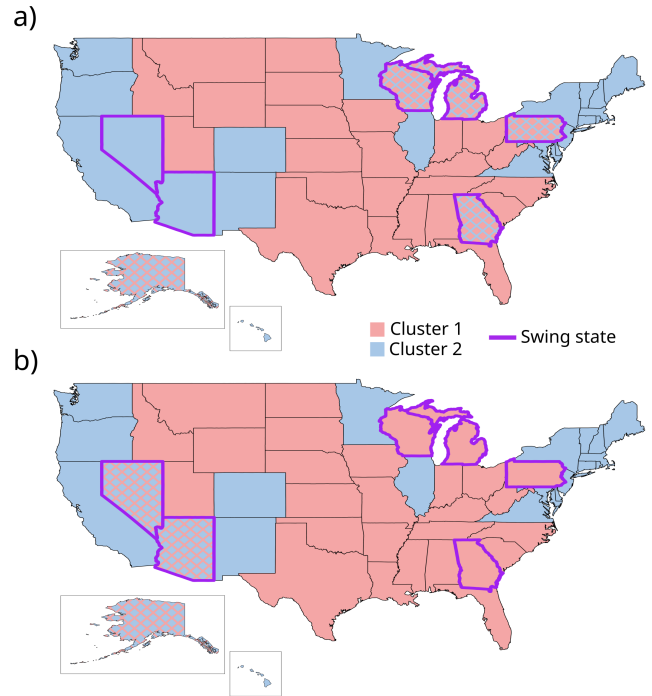


Figure 13: Clusters derived from K-means analysis based on the average reliance  $\hat{\sigma}_{s'}$  on each singleton information source and average respondents' fear score  $\phi_{s'}$  for them across U.S. states, without stratification by *Age* or *Education*. These clusters are compared with the results of the a) 2020 and b) 2024 U.S. political elections.

### Availability of materials and data

All datasets used in this work will be publicly available. Further details will be provided upon acceptance, in accordance with double-blinded submission requirements.

### Declaration of competing interest

The authors declare no competing interests.

### Funding

Further details will be provided upon acceptance, in accordance with double-blinded submission requirements.